THEORETICAL INVESTIGATION ON THE ELASTIC AND THERMODYNAMIC PROPERTIES OF $CuInS_2$

by

Shenghai FAN[a,b,c*] and Ziai LU[b*]

[a]School of Materials Engineering, Yancheng Institute of Technology, Yancheng, China
[b]College of Harbour, Coastal and Offshore Engineering, Hohai University, Nanjing, Jiangsu, China
[c]Key Laboratory for Ecological-Environment Materials of Jiangsu Province,
Yan cheng Institute of Technology, Yancheng, China

Original scientific paper
https://doi.org/10.2298/TSCI210801302F

The first-principles method based on the density functional theory is used to investigate the properties of chalcopyrite $CuInS_2$ crystal. The crystal structural parameters are optimized, and the elastic constants and bulk modulus are also calculated, and the results are highly consistent with those in the literature. The stability of the crystal is judged from the Born stability criteria. Based on the quasi-harmonic Debye model, the pressure and temperature dependencies of the bulk modulus, the Debye temperature, the Grüneisen parameter, and the thermal expansion coefficient are obtained.

Keywords: *$CuInS_2$, bulk modulus, thermodynamic properties*

Introduction

The $CuInS_2$ exists in different forms, including film, single crystal, nanocrystalline, and doped modifier. The $CuInS_2$ is a direct bandgap material with appropriate bandgap width and relatively low preparation cost, which is a potential material for preparing thin-film solar cells. Meanwhile, its non-cubic structure characterizes many useful electrical and optical properties, such as third-order nonlinear optical properties [1-3]. In the experiments, different forms of $CuInS_2$ were synthesized by different methods, and their various properties were studied [4, 5]. However, in the theoretical aspect, little research on this crystal was reported. For example, Lazewski *et al*. [6] used plane-wave pseudopotential density functional theory to optimize lattice parameters, band structure, and lattice dynamic properties of $CuInS_2$. Yamamoto and Katayamayoshida [7] studied the doping of $CuInS_2$, including the influence of P and In codoping on its energy band and structural stability. Eryigit *et al*. [8] investigated its phonon and dielectric properties. Zhao and Zunger [9] calculated the electronic structure and ferromagnetism of Mn-doped $CuAlS_2$, $CuGaS_2$, $CuInS_2$, $CuGaSe_2$, and $CuGaTe_2$ by theoretical method. Verma *et al*. [10] studied the elastic properties of a series of chalcopyrite crystals using the ion charge theory. Theoretically, there is no comprehensive data on $CuInS_2$ crystals, especially the theoretical results of mechanical and thermal properties have not been reported in detail. Therefore, this paper is focused on theoretical research about the mechanical and thermal properties of $CuInS_2$ materials.

*Corresponding authors, e-mail: dahai004@163.com; hhulza@163.com

Method and data

In this paper, the first-principles density functional theory method [11, 12] based on plane-wave pseudopotential was applied to calculate the crystal structure and elastic properties of $CuInS_2$ with the help of calculation program [13, 14]. In the calculation, Perdew-Burke-Ernzerhof of Generalized Gradient Approximation (GGA) was used for the exchange-correlation potential function [15]. The interaction between electrons and ion solids was described by Vanderbilt ultrasoft pseudopotentials [16]. Through a series of convergence tests, the *k*-points in the Brillyuan region were selected as $8 \times 8 \times 9$ Monkhorst-pack grids with truncation energy of 500.0 eV, and the total energy self-consistent convergence accuracy was set as $1.0 \cdot 10^{-6}$ eV/Atom. These parameters were used to optimize the structure of $CuInS_2$ crystal, and the most stable crystal structure with minimum energy was obtained.

Results and discussion

Crystal structure

In order to obtain good results, a stable crystal structure is necessary. The lattice constants of the stable structure of $CuInS_2$ crystal are given in tab. 1. The optimized lattice constant, *a*, is close to the experimental value of 0.5525 nm [17, 18], and the maximum error ranges of *a* and *c* are 1.13-1.23% and 1.12-1.60%, respectively. The optimized lattice constants are used in the subsequent physical property calculation.

Table 1. The lattice constants, *a* [nm], *c* [nm] of $CuInS_2$ compared to experimental and theoretical values

	a	*c*
This work	0.5588	1.1253
[17]	0.5519	1.1072
[18]	0.5525	1.1127
[8]	0.5352	1.1503
[6]	0.5722	1.2448

Elastic properties

The elastic constant is a bridge to understanding the mechanical and dynamic properties of materials. It can also be obtained by applying certain stress to the material and analyzing its strain [19, 20]. The $CuInS_2$ crystal belongs to the space group and shows tetragonal symmetry. Its elastic constant has six independent components, which can be expressed by Young's symbol as C_{11}, C_{33}, C_{44}, C_{66}, C_{12}, and C_{13}. Table 2 shows the elastic constants of $CuInS_2$ crystals calculated by density functional theory. The six independent elastic constants of chalcopyrite crystals must meet the Born mechanical stability condition [21]. That is, the elastic constants meet the following relationship:

$$C_{11}, C_{33}, C_{44}, C_{66} > 0 \tag{1}$$

$$C_{11} > |C_{12}| \tag{2}$$

$$C_{11}C_{33} > C_{13}^2 \tag{3}$$

$$(C_{11} + C_{12})C_{33} > 2C_{13}^2 \tag{4}$$

Table 2. The calculated elastic constants C_{ij} [GPa]

	C_{11}	C_{12}	C_{13}	C_{33}	C_{44}	C_{66}
This work	84.57	53.07	52.901	78.17	38.05	37.55
[7]	83.7	54.4	54.8	84.5	35	33.9
[10]	87.3	54.6	63.8	100.8	37	33.6

Substituting the elastic constants in the previous table into the Born criterion, we find that the elastic constants of $CuInS_2$ crystal meet the Born mechanical stability condition, indicating that the obtained $CuInS_2$ crystal structure is mechanically stable, which also proves that the calculated elastic constants are correct. The elastic constants of $CuInS_2$ calculated by us and the theoretical calculation results of other authors are also given in tab. 2 [7, 10]. By comparison, it is found that the elastic constants of $CuInS_2$ crystals calculated by the GGA approximation method under the density-functional framework adopted by us are in good agreement with the theoretical calculation results of other authors. Using these elastic constants C_{ij}, the elastic anisotropy factor of $CuInS_2$ crystal can be calculated:

$$\alpha_1 = \frac{2C_{44}}{C_{11} - C_{12}} = 2.42 \tag{5}$$

$$\alpha_2 = \frac{C_{66}}{C_{44}} = 0.99 \tag{6}$$

The calculated results show that there is a significant difference between them, indicating that $CuInS_2$ crystal has strong anisotropy, and the calculated anisotropy factor values are highly consistent with other theoretical results in tab. 3 [7, 10].

Table 3. The two anisotropic factors a_1 and α_2, linear and volume compressibilities χ_a, χ_c, χ [TPa^{-1}], the bulk modulus B [GPa], the shear modulus G [GPa], Young's modulus E [GPa], and Poisson ratio σ of $CuInS_2$

	a_1	α_2	χ_a	χ_c	χ	B	G	E	σ
This work	2.42	0.99	4.9	5.9	15.7	63.34	25.55	68.39	0.320
[7]	2.35	0.98	5.24	5.04	15.52	64.4	24.52	65.28	0.331
[10]	2.26	0.91	6.00	2.32	14.33	70.44	27.23	72.37	0.329

Based on the knowledge of elastic constants, the linear compressibility χ_a, χ_c, and the volume compressibility, χ, of crystals along axis a and c can be further calculated. The calculated results and other theoretical values are listed in tab. 3. Where χ_a, χ_c, and χ are expressed, respectively:

$$\chi_a = -\frac{1}{a}\frac{\partial a}{\partial p}|_{p=0} = \frac{c_{33} - c_{13}}{c_{33}(c_{11} + c_{12}) - 2c_{13}^2} \tag{7}$$

$$\chi_c = -\frac{1}{c}\frac{\partial c}{\partial p}|_{p=0} = \frac{c_{11} + c_{12} - 2c_{13}}{c_{33}(c_{11} + c_{12}) - 2c_{13}^2} \tag{8}$$

$$\chi = -\frac{1}{V}\frac{\partial V}{\partial P}|_{p=0} = 2\chi_a + \chi_c \tag{9}$$

The calculation results show that the two linear compressibilities and volume compressibility along with the crystal axis *a* and *c* are more consistent with the results calculated by Yamamoto and Katayamayoshida [7]. The results illustrate that the effect of external pressure on the axis *a* and *c* compression of the crystal is consistent.

Theoretically, the elastic modulus and shear modulus can be expressed by Voigt and Reuss [22, 23] approximation methods. The bulk modulus of $CuInS_2$ single crystal is expressed by Voigt approximation:

$$B_V = \frac{1}{9}(2C_{11} + C_{33} + 2C_{12} + 4C_{13}) \tag{10}$$

Reuss approximation uses the combination of elastic constants to represent the bulk modulus [24, 25]:

$$B_R = \frac{(C_{11} + C_{12})C_{33} - 2C_{13}^2}{C_{11} + C_{12} + 2C_{33} - 4C_{13}} \tag{11}$$

The Voigt of shear modulus G of $CuInS_2$ single crystal can be approximated:

$$G_V = \frac{1}{15}(2C_{11} + C_{33} - C_{12} - 2C_{13} + 6C_{44} + 3C_{66}) \tag{12}$$

Reuss shear modulus can be approximated:

$$G_R = 15\left[\frac{18B_V}{C^2} + \frac{6}{C_{11} - C_{12}} + \frac{6}{C_{44}} + \frac{3}{C_{66}}\right]^{-1} \tag{13}$$

where $C^2 = (C_{11} + C_{12})C_{33} - 2C_{13}^2$, G_V – the Voigt shear modulus, and G_R – the Reuss shear modulus. In practical application, Hill [26] believes that the bulk modulus and shear modulus of materials should be the average value of the previous two approximation methods, namely:

$$B = \frac{1}{2}(B_V + B_R) \tag{14}$$

$$G = \frac{1}{2}(G_V + G_R) \tag{15}$$

The bulk modulus and Shear modulus obtained by Hill's method are in good agreement with other theoretical values in tab. 3, which also proves the accuracy of the calculation. We use *B* and *G* values to calculate the Poisson's ratio of materials:

$$\sigma = \frac{3B - 2G}{6B + 2G} = 0.320 \tag{16}$$

Young's modulus of $CuInS_2$ crystal can also be calculated using *B* and G:

$$E = \frac{9BG}{3B + G} \tag{17}$$

According to Pugh's [27] criterion, when the ratio of *B*/*G* is less than 1.75, the material is considered brittle, otherwise, it is extended. The calculated $CuInS_2$ crystal *B*/*G* = 2.48, indicating that $CuInS_2$ crystal is a ductile material.

Thermodynamic properties

First, a series of lattice constants were selected to calculate the corresponding protocell volume and total energy of $CuInS_2$ and obtain *E*-*V* data. Birch-Monaghan [28] state

equation was used for fitting, as shown in fig. 1. The following calculation is done by GIBBS program [29]. The thermodynamic properties of $CuInS_2$ crystals in the range of pressure 0-50 GPa and temperature 0-1000 K have been calculated.

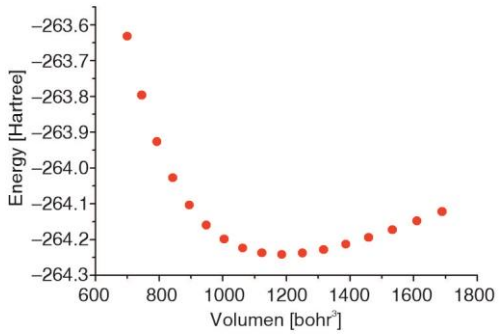

Figure 1. Total energy *vs*. volume of $CuInS_2$ crystal

The bulk modulus B and the first derivative of bulk modulus B` of bulk modulus with respect to pressure of $CuInS_2$ crystal were obtained by fitting. The values of the fitted lattice constants a and c are 0.5595 nm and 1.1266 nm, respectively, which agree with the experimental and theoretical values given in tab. 1. The bulk modulus B = 65.9 GPa and the first derivative of bulk modulus with respect to pressure B` = 4.73. The bulk modulus B is also in good agreement with the theory in tab. 3, which further proves the correctness of the calculated results.

Figure 2 shows the relationship between bulk modulus B and temperature T = 0-1000 at zero pressure, when T < 100 K, B remains almost constant, and T > 100 K, B decreases sharply as the temperature increases. B and T are fitted into a third-order polynomial, and the following relationship can be obtained:

$$B = 65.49399 - 0.00242T - 2.94997 \cdot 10^{-5} T^2 + 4.13811 \cdot 10^{-8} T^3$$

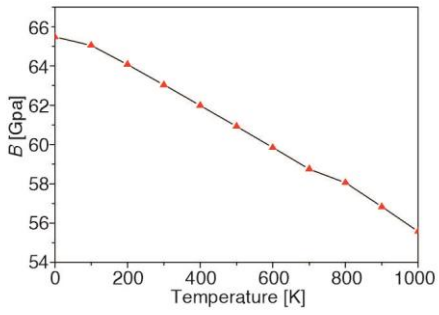

Figure 2. Bulk modulus B as a function of T at P = 0 GPa

Debye temperature can be applied to describe the physical properties of substances, and different substances have different Debye temperatures. Table 4 shows Debye temperatures of $CuInS_2$ crystals at different pressures and temperatures. According to the analysis of the data in the table, Debye temperature, Θ, decreases gradually with the increase of temperature when the pressure is 0, 10, 20, 30, 40, and 50 GPa, respectively, decreasing 10.33%, 6.16%, 4.31%, and 3.18%, respectively. It can be concluded that the higher the pressure, the less the influence of temperature on Θ.

In crystal lattice vibration, the Grüneisen parameter, γ. can not only represent the anharmonic interaction in the crystal but also reflect the dependence of Debye temperature, Θ, and crystal volume. Through the Grüneisen parameter, γ, many anharmonic properties of materials can be predicted, such as thermal expansion coefficient, acoustic frequency, and the relationship between line width and temperature, *etc*. The Grüneisen parameters, γ, of $CuInS_2$ crystals at different temperatures (0, 200, 400, 600, 800, and 1000 K) and different pressures (0, 10, 20, 30, 40 and 50 GPa) are shown in tab. 4. The analysis shows that for a given pres-

sure, the Grüneisen parameter, γ. increases gradually with the increase of temperature. When the temperature is 0, 200, 400, 600, 800 and 1000 K, respectively, γ decreases with the change of pressure (0-50 GPa) in turn 21.22%, 21.5%, 21.97%, 22.47%, 22.95%, and 23.28%.

Table 4 Debye temperature, Θ [K] and Grüneisen parameter, γ, of the $CuInS_2$ at temperatures *T* [K] and pressures *P* [GPa]

T [K]	*P* [GPa]	0	10	20	30	40	50
0	Θ	321.22	407.52	472.17	525.31	571.16	612.73
	γ	2.186	1.958	1.856	1.795	1.753	1.722
200	Θ	318.90	406.21	471.18	524.54	570.55	612.23
	γ	2.192	1.960	1.857	1.795	1.754	1.722
400	Θ	314.62	403.49	468.90	522.59	568.87	610.76
	γ	2.208	1.966	1.860	1.797	1.755	1.723
600	Θ	310.05	400.54	466.41	520.43	566.99	609.99
	γ	2.225	1.972	1.863	1.799	1.757	1.725
800	Θ	306.38	397.51	463.88	518.23	565.05	607.29
	γ	2.240	1.978	1.867	1.802	1.758	1.726
1000	Θ	303.65	395.98	462.60	517.72	564.07	606.39
	γ	2.251	1.981	1.868	1.803	1.759	1.727

The relation of α-T of materials is similar to that of C_V-T. The relationship between the thermal expansion coefficient of $CuInS_2$ and temperature and pressure. The α-T is similar to C_V-T curve as shown in fig. 3. At low temperature, the thermal expansion coefficient, α, increases in proportion to T^3, while at high temperature, it gradually increases in a linear relationship and eventually tends to be constant. In addition, the coefficient of thermal expansion α varies greatly with temperature (the reason is the anharmonic force between atoms) at low pressure.

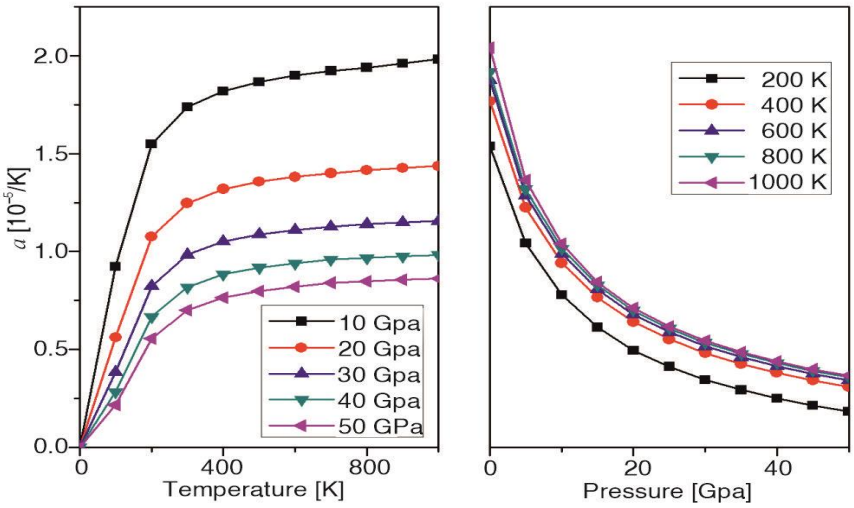

Figure 3. Pressure and temperature dependence of the thermal expansion coefficient α

Conclusion

The crystal structure and elastic properties of $CuInS_2$ were systematically studied by the first-principles method. The equilibrium structure parameters of $CuInS_2$ crystal are obtained by optimizing the system, and the calculated results are in good agreement with the experimental and theoretical values. According to the calculated elastic constant C_{ij} of $CuInS_2$ crystal, Voigt-Reuss-Hill (VRH) approximation method was used to calculate a series of physical parameters such as bulk modulus, B, and Poisson's ratio, σ, to describe the mechanical properties of $CuInS_2$ crystal. The Birch-Murnaghan equation of state was applied to fit the E-V curve, and the quasi-harmonic Debye model was used to study the thermodynamic properties of $CuInS_2$ crystals with chalcopyrite structure. In the range of pressure 0-50 GPa and temperature 0-1000 K, Debye temperature, Θ, thermal expansion coefficient, α, and Grüneisen parameter, γ. of $CuInS_2$ crystal were calculated with changing temperature or pressure.

References

[1] Du, J. J., *et al*., Research Progress of CIS (CIGS) Membrane Materials, *Materials Review*, *21* (2007), 4, pp. 9-12
[2] Li, J., *et al*., Preparation of $CuInS_2$ thin Films by Single-Step Electrodeposition (in Chinese), *Acta Phys Chim Sin*, *25* (2009), 12, pp. 2445-2449
[3] Sun, Q., *et al*., Preparation of $CuInS_2$ Semiconductor thin Films by Electrodeposition and their Optical Properties, *Journal of Artificial Crystals*, *42* (2013), 1, pp. 65-71
[4] Wang, Z. D., *et al*., Preparation and Properties of $CuInS_2$ thin Films by Single Source Thermal Evaporation, *Vacuum*, *48* (2011), 1, pp. 29-32
[5] Feng, L., *et al*., Study on the Structure, Morphology and Optical Properties of $CuInS_2$ Nanocrystals, *Journal of Chemical, 69* (2011), 23, pp. 2870-2876
[6] Lazewski, J., *et al*., Band Structure, Born Effective Charges and Lattice Dynamics of $CuInS_2$ from Ab Initio Calculations, *Journal of Chemical Physics, 117* (2002), 6, pp. 2726-2731
[7] Yamamoto, T., Katayamayoshida, H., A Codoping Method in $CuInS_2$ Proposed by Ab Initio Electronic Structure Calculations, in: *Tetnary and Multinary Compounds*, CRC Press, Boka Raton, Fla., USA, 1998, pp. 37-40
[8] Eryigit, R., *et al*., Ab Initio Vibrational and Dielectric Properties of Chalcopyrite $CuInS_2$, *European Physical Journal B*, *33* (2003), 3, pp. 251-254
[9] Zhao, Y. J., Zunger, A., Electronic Structure and Ferromagnetism of Mn-Substituted $CuAlS_2$, $CuGaS_2$, $CuInS_2$, $CuGaSe_2$ and $CuGaTe_2$, *Physical Review B, 69* (2004), 10, pp. 104422-104428
[10] Verma, A. S., *et al*., Elastic Properties of Chalcopyrite Structured Solids, *Materials Chemistry and Physics*, *132* (2012), 2, pp. 416-420
[11] Hohenberg, P., Kohn, W., Inhomogeneous Electron Gas, *Physical Review*, *136* (1964), 3B, B864-B871
[12] Kohn, W., Sham, L. J., Self-Consistent Equations Including Exchange and Correlation Effects, *Physical Review, 140* (1965), 4A, pp. A1133-A1138
[13] Payne, M. C., *et al*., Iterative Minimization Techniques for Ab Initio Total-Energy Calculations: Molecular Dynamics and Conjugate Gradients, *Reviews of Modern Physics*, *64* (1992), 4, pp. 1045-1097
[14] Milman, V., *et al*., Electronic Structure, Properties, and Phase Stability Of Inorganic Crystals: A Pseudopotential Plane-Wave Study, *International Journal of Quantum Chemistry*, *77* (2000), 5, pp. 895-910
[15] Perdew, J. P., *et al*., Generalized Gradient Approximation Made Simple, *Physical Review Letters*, *77* (1996), 18, pp. 3865-3868
[16] Vanderbilt, D., Soft Self-Consistent Pseudopotentials in a Generalized Eigenvalue Formalism, *Physical Review B*, *41* (1990), 11,pp. 7892-7895
[17] Hahn, H., *et al*., *Zeitschrift fur Anorganische und Allgemeine Chemie*, *271*(1953), pp.153-170
[18] Abrahams, S. C., Bernstein, J. L., Piezoelectric Nonlinear Optic $Cugas_2$ And $Cuins_2$ Crystal Structure: Sublattice Distortion in $A^{I}B^{III}C\ V^{I}_2$ and $A^{II}B^{IV}C^{V}_2$ Type Chalcopyrites, *Journal of Chemical Physics*, *59* (1973), 10, pp. 5415-5422
[19] Karki, B. B., *et al*., Structure and Elasticity of MgO at High Pressure, *American Mineralogist, 82* (1997), Feb., pp.51-60

[20] Wentzcovitch, R. M., *et al*., Ab Initio Study of $MgSiO_3$ and $CaSiO_3$ Perovskites at Lower-Mantle Pressures, *Physics of the Earth and Planetary Interiors,* 90 (1995), 1-2, pp. 101-112
[21] Born, M., Huang, K., *Dynamical Theory of Crystal Lattices*, Clarendon Press, Oxford, UK, 1954
[22] Voigt, W., *Lehrbuch der Kristallphysik*. Teubner Verlag, Leipzig, 1928
[23] Reuss, A., Berechnung der Fliessgrenze von Mischkristallen auf Grund der Plastizitätsbedingung für Einkristalle, *Zeitschrift für Angewandte Mathematik und Mechanik, 9* (1929), pp. 49-58
[24] Reuss, A., Calculation of the Flow Limits of Mixed Crystals on the Basis of the Plasticity of Mono-Crystals, *Journal of Applied Mathematics and Mechanics*, *9* (1929), pp. 49-58
[25] Mehl, M. J., *et al*. Structural Properties of Ordered High Melting Temperature Intermetallic Alloys from First-Principles Total-Energy Calculations, *Physical Review B, 41* (1990), 15, pp. 10311-10323
[26] Hill, R., The Elastic Behaviour of a Crystalline Aggregate, *Proceedings of the Physical Society Section A, 65* (1952), 5, pp. 349-354
[27] Pugh, S. F., Relations Between the Elastic Moduli and the Plastic Properties of Polycrystalline Puremetals, *Philosophical Magazine, 45* (1954), 367, pp. 823-84
[28] Birch, F., Finite Elastic Strain of Cubic Crystals, *Physical Review, 71* (1947), pp. 809-824
[29] Blanco, M. A., *et al*., GIBBS: Isothermal-Isobaric Thermodynamics of Solids from Energy Curves Using a Quasi-Harmonic Debye Model, *Computer Physics Communications*, *158* (2004), 1, pp. 57-72

Paper submitted: August 1, 2021
Paper revised: October 13, 2021
Paper accepted: October 13, 2021